Chapter - 4

Experimental Analysis with Various Designs of Branched Flagella

4.1 Introduction

In the previous chapter test rig for scaled up branched flagella was designed with objective to study propulsive force generation of planar motion of swimmer. In the present chapter, we first discuss about the swimming micro-organism and their propulsion through cilia and flagella, various types of flagella and their performance. Next, the macro-scale experiments performed by different researchers [1]-[7] with different types of flagella is addressed. Later, Taguchi analysis design of experiment (DOE) is attempted on various branched flagellated swimmer by varying number of branches, orientation of branches and spacing between branches on flagella surface. The effect of environmental parameters such as viscosity of fluid medium and speed of motor on propulsive force generation is also studied.

Flagellum is spiral filaments made up of flagellin protein subunit that emerges from cell surface of eukaryotic and prokaryotic cells. The word flagellum means 'whip'. The prime role of flagellum is to propel bioorganism bearing flagella but it also works as sensory organelle, being perceptive to external stimuli such as chemical, light and temperature from outside the cell [1],[2]. Both eukaryotic and prokaryotic flagella help in locomotion but vary in protein composition, structure and mechanism of propulsion.

Prokaryotic flagellum rotates at 100 Hz to 500 Hz and driven by proton movement while eukaryotic flagella rotate at 25 Hz to 45 Hz bends and propel by adenosine triphosphate (ATP). Prokaryotic flagella have stator and rotor like electric motor. It is semi-flexible; having rotor that moves cells either clockwise or anticlockwise in the form of bundle by pushing against fluidic environment. A clockwise movement propel the cells forward while anticlockwise motion leads to backward propulsion. The basal body acts as universal joint for complete rotation of rotating flagella. Eukaryotic cells move by utilizing energy from ATP while the mechanism of propulsion in prokaryotic cells is due to flow of ions across the membrane (proton motive force) and act as

circuit element i.e. capacitor. Prokaryotic flagella are comparatively less in diameter than eukaryotic flagella. *E. coli* is the well-known example of prokaryotic bacteria exists in nature having rod shaped helical filaments connected to motor protein. It rotates in anticlockwise (forward) and clockwise (backward) direction.

Table 4.1: Geometric dimensions of eukaryotic and prokaryotic flagella [3]

	Eukaryotic Flagella	**Prokaryotic Flagella**
Length (μm)	50-300	1-15
Diameter (μm)	10-100	0.1-5

Eukaryotic cilia and flagella are structurally similar but differ in performance and length. In eukaryotes an interchangeable name is used for cilia and flagella. If filaments are shorter in length and larger in numbers, cilia name is used for eukaryotic cells. Flagella name is given to eukaryotic cell if filament is longer and only one or two is present on the surface of it. The beating pattern of eukaryotic cilia and flagella is different rather same in structural form. Flagella show planar motion while cilia exhibit three dimensional power and recovery stroke during motion. *Paramecium* is one of the examples of eukaryotic cell in which cilia is present on the surface and used for locomotion inside fluidic medium. In the oviduct of female a large number of cilia are present in the form of array to move eggs. Sperm cell is an example of eukaryotic flagellated cell which utilizes its flagellum to travel through female reproductive tract. Researchers are utilizing flagella to design artificial swimmer while cilia design is explored for mixing of fluid at micron/ nano level [4].

Flagellar arrangement is classified as per different species of bacteria (Figure 4.1) such as single flagellum (Monotrichous bacteria; e.g. *Vibrio cholera* bacterial pathogen), multiple flagellum (Lophotrichous bacteria; e.g. *Pseudomonas aerugoinosa*), single flagellum on two opposite ends (Amphitrichous bacteria; *Spirillum minor*), flagella emerges in all directions (Peritrichous bacteria; *E. coli*) [13]. Monotrichous, lophotrichous and amphitrichous bacteria have flagella at the ends of the cells and considered as polar flagella. In literature, various theories have been developed and investigation has been performed on monotrichous, amphitrichous and lophotrichous flagellar arrangement. Experimental studies have been performed at scaled up level

through planar as well as helical motion using different types of flagellar arrangements presented in subsequent section chronologically showing their dimensional parameters.

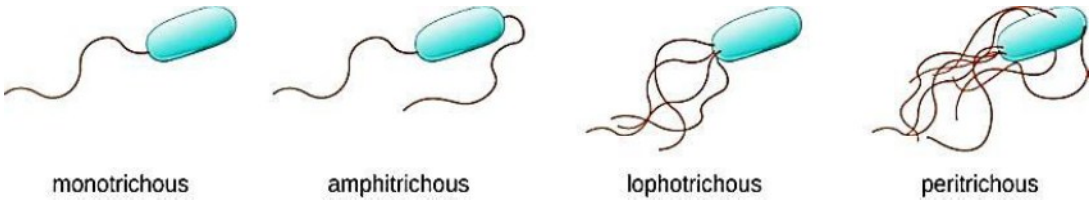

Figure 4.1: Different arrangements of flagella of flagellated bacteria [5]

4.2 Literature Review: Macro Scale Flagellum Designs

Important part in designing of test rig is to design flagellum. Different types of flagella were proposed and designed by researchers for swimming micro-robots. In 1996, Honda et al. attached small cubic $SmCo_5$ magnet to the copper spiral wire as shown in Figure 4.2. Four parameters were considered for designing the copper spiral wire as flagella i.e. *2b*, λ, *2a* and *L* where, *2a* is the diameter and *L* is the length of wire, *2b* and λ are diameter and linear wavelength of wire as shown in Figure 4.2. The wire diameter was fixed and other dimensional parameters were varying to see the effect on propulsive velocity [6].

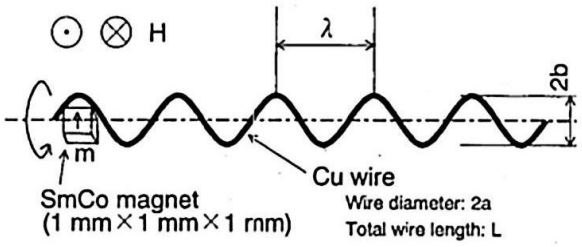

Figure 4.2: Shows copper wire as helical flagella [6]

In 2005, Behkam and Sitti [7] validated the mathematical modelling of nanoswimmer with experimental investigation carried out at scaled up level. Buckingham Pi theorem is being utilized to choose the suitable dimensions to ease the fabrication process of designed flagellated swimmer. A steel wire of 1.23 mm in diameter was used as scaled up flagella having helical diameter and pitch of 14.8 mm and 14.7 mm as shown in Figure 4.3. The fabricated flagellum was submerged in silicon oil of viscosity 350 cSt.

Experiments were performed for two sets of flagella but having different lengths (L_1- 5.60 cm and L_2- 6.20 cm).

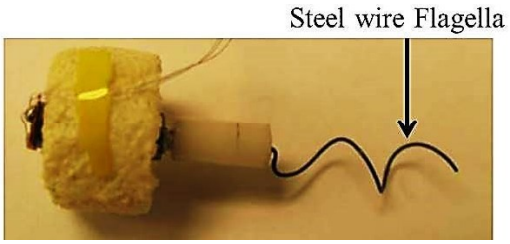

Figure 4.3: Macro-scale helical flagella made up of steel wire [7]

In 2006, Tony et al.[8] designed a robotic swimmer shown in Figure 4.4 and gave its name as Robo-Chlam after algae *chlamydomonas*. Stainless steel wires of length 18 cm to 30 cm are used as flexible flagella. Two different diameters 0.5 mm and 0.61 mm of flagella have been taken for experiments which resulted in bending stiffness $6.1x10^{-4}$ and $1.3x10^{-3}$ Nm^2. Through experimental data, it was observed that flagella having smaller length move stiffly in comparison to flagella having larger in length.

Figure 4.4: Flexible steel wire designed for planar propulsion [8]

In 2007, Kosa et al. [9], designed a propulsion system by fabricating tail of swimmer using piezoelectric material. The swimming tail was divided into three segments and travelling wave has been created to propel it. Same signal amplitude was applied to each piezoelectric segment with phase difference. The length of tail is 35 mm on which 31 mm long and 0.2 mm thick PZT piezoelectric element has been coated. Tail moves by 8 mm when actuator is activated. In succeeding work in 2008, Kosa et al.[10] mentioned the decrement in propulsive force on attaching the head to the swimming tail.

In 2009, Coq et al. [11] fabricated the elastic filament of polyvinylsiloxane polymer mixed with its curing agent in a ratio of 1:1 and placed at room temperature after thermally activating it. The dimensions of fabricated filament having radius 0.435 mm and length is varied from 2 to 10 cm, immersed in glycerine filled tank of viscosity 1Pas.

A motor has been placed on the top of the tank and providing the rotation to filament by varying speed of motor from 0.1 RPM to 10 RPM.

In 2010, Ha and Goo [12] designed a biomimetic prototype shown in Figure 4.5. A helical aluminium wire having diameter 0.5 mm and length 27 mm has been used as filament which is connected to DC motor through coupler. Fountain et al. (2010) [13] created various types of macro-scale helical magnetic microrobot made of NdFeB as shown in Figure 4.6 of length 3.175 mm and diameter 1.625 mm and observed its movement inside water filled chamber.

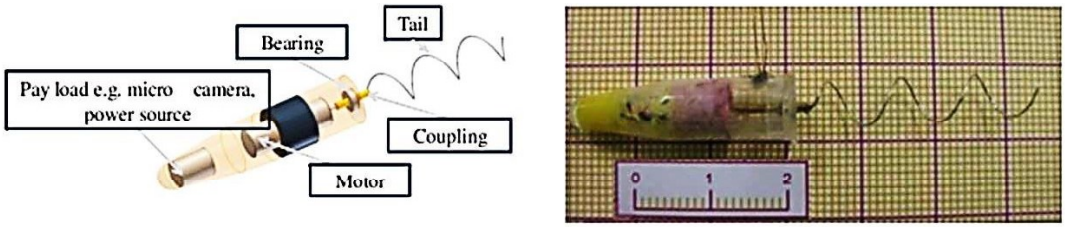

Figure 4.5: Aluminium wire as helical flagella is shown [12]

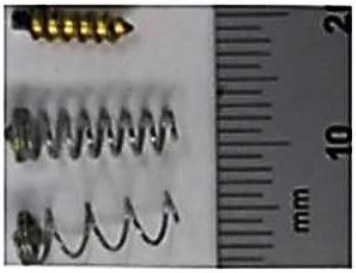

Figure 4.6: Steel wire spring is wrapped on NdFeB magnet [13]

In 2011, Singleton et al. [14], performed scaled up experiments with multi-flagellar helical swimmer. The different designs of flagella are shown in Figure 4.7 having flexible helices, stiff helices and straight flexible rod. The helices of flagella are having length 15.40 mm, wavelength 5.10 mm and amplitude 1.88 mm. Only vertical motion is followed by rotating it through external magnetic-field, connected to cantilever beam. Increment in thrust/propulsive force has been observed for system having two helices than single helix. The main objective of their work is to compare the performance of each fabricated design of flagella rather than computing exact value of torque and thrust force.

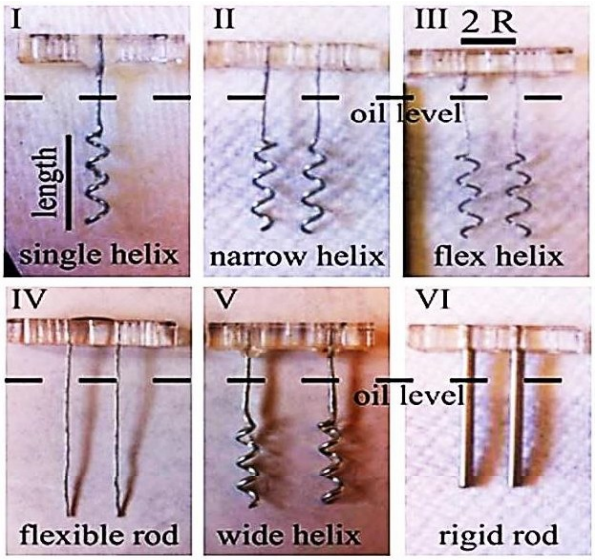

Figure 4.7: Arrangement of different helical flagella [14]

In 2011, Temel et al. [15] designed two robot as shown in Figure 4.8 having different dimensions of length 2.45 mm and 2.17 mm, radius 180 μm and 230 μm. Head of the microrobot is made up of permanent magnet NdFeB and helical tail is made up of metal wire that moves in the presence of rotating magnetic-field inside glass pipette filled with glycerol (0.1 Pas) and water (0.001 Pas). Maximum speed 3.5 mms^{-1} has been observed for 2.45 mm long microrobot at 7.60 mT rotating field. Two findings for smaller head and long tail helical robots are, (1) for smaller head, drag force become smaller which increases the speed of the robot, (2) longer helical tail with more turns increases the speed of the robot.

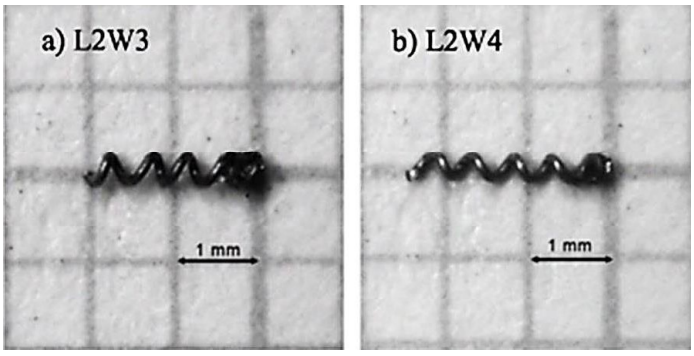

Figure 4.8: Metal wire helical flagella (a) shorter and thicker, (b) longer and thinner, having magnetic head [15]

In 2014, Xu et al. [16] studied different propulsive characteristics such as swimming velocity of scaled up magnetic helical filament having various shapes of head shown in Figure 4.9. The length of scaled up helical nanobelts (SHN) has been chosen 10 cm. A different head shape is attached on SHN such as cylindrical head, square head and spherical head. One design of SHN consists of ABSPlusP400 by rapid prototyping machine and covered with NdFeB magnet, second design consists of titanium and coated with ferromagnetic material such as Nickel and having length 2 cm.

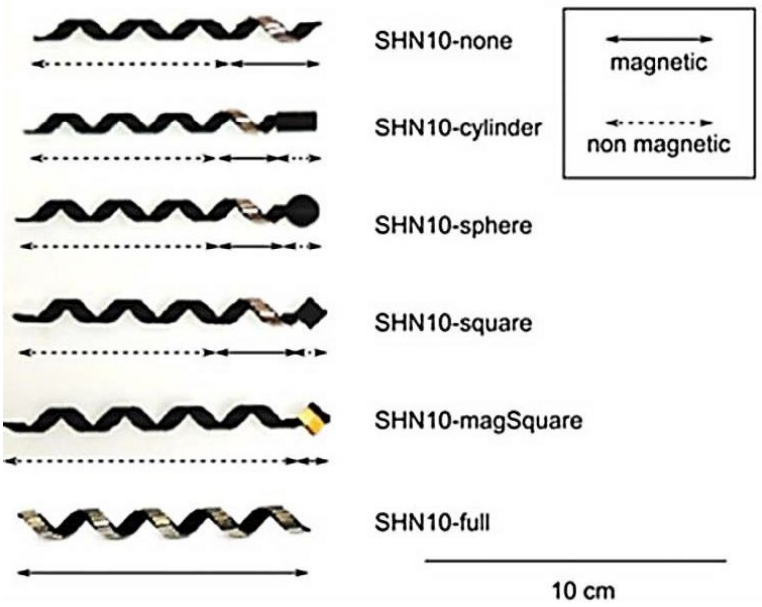

Figure: 4.9: Scaled up helical nanobelts with different shapes of head attached [16]

In 2014, Ye et al. [17] studied increase in propulsive speed on adding straight flexible flagella up to 4 in number. It is mentioned in literature that as long as the Reynolds number is same for different scale geometry, flow pattern remain same for the system and it is being utilized to study hydrodynamic interaction for two different scaled systems. Magnetically planar multi-flagella have been fabricated through soft-lithography shown in Figure 4.10. Three sets of multi-flagella system is made with different dimensions and material; 1) Cylindrical head (diameter 500 μm and height 600 μm) with flagella length 1.5 mm, width 120 μm , thickness 100 μm and made up of ST-1087 (Elastic modulus E 9.8 MPa); 2) Flagella length 1 mm, width 60 μm , thickness 50 μm along with same cylindrical head and made up of ST 1060 (Elastic modulus E 2.9 MPa) and; 3) Flagella length 1 mm ST 1060 (E 2.9 MPa) with same width and thickness as set 2 design attached with cylindrical head (diameter 180 μm and height 700 μm). A

rotating magnetic-field of 12 mT was used to generate swimmer propulsion. A minimum change has been noticed on changing the dimensions of flagella while increasing the number of flagella leads to significant increase in swimming velocity. The measurements in lesser viscous medium have not been preferred such as water because swimmer get sink into medium before any significant measurement.

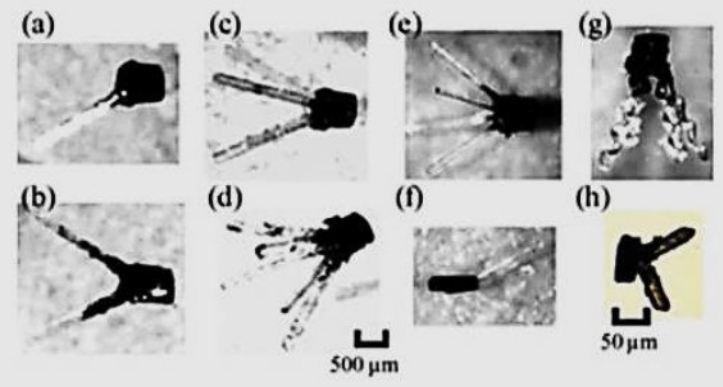

Figure 4.10: Multi-flagella design of robots with different dimensions of head and tail [17]

In 2015, Temel and Yesilyurt [18] investigated the biomimetic millimetre size swimmer having cylindrical magnetic head inside rectangular channel filled with glycerol (viscosity 1.412 Pas). The helical swimmer is created from thin copper wire by stretching it. NdFeB magnet is used as magnetic head in cylindrical shape and attaching it with helical tail. Length of helical tail is 1.1 mm, diameter 0.09 mm and diameter of the cylinder body 0.4 mm, length of cylinder body 0.8 mm.

In 2017, Wang et al. [19], investigated the forward and backward motion through single end and double end helical swimmer shown in Figure 4.11. It is difficult to measure the propulsive force of micron size swimmer because of that a scaled up millimeter size swimmer has been fabricated. A cylindrical magnetic head is used and fixed at one end of swimmer (tungsten wire). They designed double helical swimmer by inspiring through amphitrichous bacteria by attaching helix at two ends of magnetic head. It generates the symmetry in movement of backward and forward motion. Length of magnetic head (NdFeB) was 0.4 mm and diameter 0.8 mm, helix radius 0.4 mm, wire radius 0.075 mm, total helical length was 5 mm.

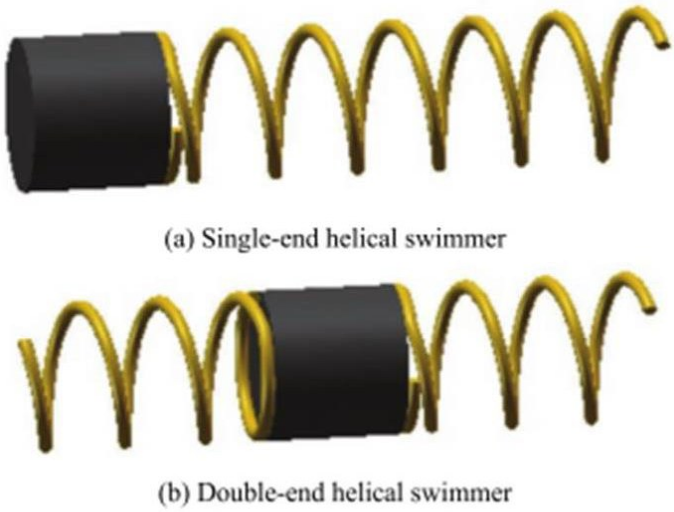

Figure 4.11: Single end and double end helical swimmer [19]

The propulsive characteristics such as thrust force and swimming velocity of flagella, achieved till now through scaled up experiments is presented in Table 4.2. In the next section, the study attempted in the field of flagella bearing hair like structure namely mastigonemes is discussed. Few attempts have been made in the field of mastigonemes bearing flagella, so there is a lot of scope to work on it.

Table 4.2: Salient work done to measure propulsive characteristics of flagella attempted in literature to date

Year/Author	Mode of Propulsion/ Medium	Geometric dimensions	Results
1996-Honda et al. [6]	Helical/Silicon oil (10St-100St)/ Re<1	$SmCo_5$ magnet (1mm×1mm×1mm) attached to spiral copper wire with diameter 0.15 mm and length 21.7 mm placed horizontally inside the tube filled with silicon oil.	Swimming velocity increases on increasing the beating frequency as well as on increasing length of copper wire.
2005-Behkam and Sitti [7]	Helical/Silicon Oil (350cSt)	Steel wire: Length 5.60 cm and 6.20 cm, diameter 1.23 mm which is mounted perpendicular to the	Thrust force generated by rotating flagella was increasing linearly with frequency in the range of

Year/Author	Mode of Propulsion/ Medium	Geometric dimensions	Results
		cantilever beam.	5 mN to 26mN
2006-Tony et al. [8]	Planar/Silicon Oil (3.18 Pas)	Stainless steel wire: Length 18cm to 30cm, diameter 0.5mm and 0.61mm, Bending stiffness 6.1×10^{-4} and 1.3×10^{-3} Nm^2	First time experimentally investigated the planar mode of propulsion at macro scale. Through experimental data it was observed that flagella having smaller length move stiffly in comparison to flagella having larger in length.
2007-Kosa et al. [9]	Planar/Gear Oil (607.6 cP)	Piezoelectric unimorph Si-PZT actuator: Length 35 mm, width 2.5 mm and thickness 0.6 mm	Thrust force measured was approximately 0.04 mN.
2008-Kosa et al. [20]	Planar/Water	Magnetic coil tail wounded using copper magnet wire of length 21 mm	The swimming tail moves backward and forward with propulsive force of 5.7 μN and 10.3 μN.
2010-Ha and Goo [12]	Helical/Silicon oil (350 cSt)	Aluminium wire: Length 27 mm, diameter 0.5 mm	The swimming velocity was observed approximately 15 mm/s.
2011-Singleton et al. [14]	Helical/Silicon Oil (30000 cSt)	Steel Spring: Length 15.40 mm	Thrust force observed for different designs was 1 mN to 16 mN.
2011-Erman and Yesilyurt [21]	Helical/Silicon oil (0.0056 Pa.s)	Steel wire: Diameter 1mm, Length 48 mm	12 different rigid helical tail is characterized for propulsive velocity in the range of 0.28 mm/s to 10.7 mm/s.
2013-Rodenborn et al. [22]	Helical/Silicon oil(100 Kg/ms)	Helical stainless steel flagella: Length 130±5 mm and radius 6.3±0.4 mm	By varying the pitch of helical macroscopic flagella, they observed thrust force, drag and torque as 80 mN, 66 mN and 6 mNm.
2014-Ye et al. [17]	Helical/Silicon oil (5 cSt and 350 cSt)	NdFeB-Polyurethane-PDMS (straight) with Young's modulus 2.9 MPa and 9.8 MPa and length of flagella are 1mm and 1.5 mm.	Numerically computed the thrust force approximately up-to 6 μN.
2019-Danis	Helical/Silicon	Steel wire- 10 mm pitch	Generated thrust force

Year/Author	Mode of Propulsion/ Medium	Geometric dimensions	Results
et al. [23]	oil (350 cSt and 30000 cSt)	length and 6.25 mm helix diameter	approximately 1 mN.
2019- Nain et al. [24]	Planar/Silicon oil (350 cSt, 10000 cSt, 15000 cSt and 20000 cSt)	PDMS Biocompatible flagella- Length 15 cm, diameter 1 cm	Observed thrust force approximately 7 mN.

4.3 Literature on Investigation on Mastigonemes Enduring Flagella

Scientist investigated the single flagella and multi-flagella system to study the increase in propulsive characteristics name as thrust force and swimming velocity at scaled up level which is discussed in the previous section. Mastigonemes presents on flagella are gaining attention of researchers because of different microorganisms present in nature are having mastigonemes such as algae, fungi and sponges. Mastigonemes are categorized into two groups on the basis of its function [25]. First, by increasing the effective surface area of flagellum and leads to increase in overall thrust force of flagella [26] such as fibrous mastigonemes (*Chlamydomonas and Ochromonas)* [27]; secondly, the mastigonemes reverses the thrust force of flagellum namely tubular mastigonemes [28]. Fibrous mastigonemes presents on both long and short flagella, is having diameter 50-100 A° and 1-3 μm long and; (2) Tubular mastigonemes is found only on long flagellum and is 200 A° in diameter and 1 μm long and creates a roughness on smooth flagellum surface. Pantonematic name is given to micro-organism if there mastigonemes arrangement is rigid enough and present in two rows; if there is single row of mastigonemes then it is stichonematic flagellum; single filament is present in acronematic flagella and two or more rows of mastigonemes along with terminal filament is present in pantacronematic flagellum [26]. In 1971, Bouck [25] studied the structure, composition and assembly of fibrous mastigonemes. A photograph of flagellum consisting of fibrous mastigonemes shows that wave propagation is planar and more efficient than helical wave motion.

In 1996, Monoclonal antibody to mastigonemes (mAb-MAST1) has been utilized to confirm the flagellar mastigonemes through immunofluorescence microscopy and transmission electron microscopy [29], [28]. Electron-micrograph is used by researchers to study size, arrangements and number of mastigonemes. Through mAb-MAST1,

researchers tested the effect of mastigonemes on flagellar motion [29]. In *ochromonas* and *chlamydomonas reinhardtii,* mastigonemes are present towards distal end of flagella at $2/3^{rd}$ to $3/4^{th}$ length of flagellum and enhancement of movement of flagellum bearing mastigonemes is being observed by increasing the effective surface area. Mastigonemes are uniform in shape and size along the surface of flagellum [29], [30]. In literature it was mentioned that mastigonemes present in *ochromonas* are more or less emerges perpendicular to the flagellum surface [28] and exhibit planar wave propulsion from base to the tip along the flagella length.

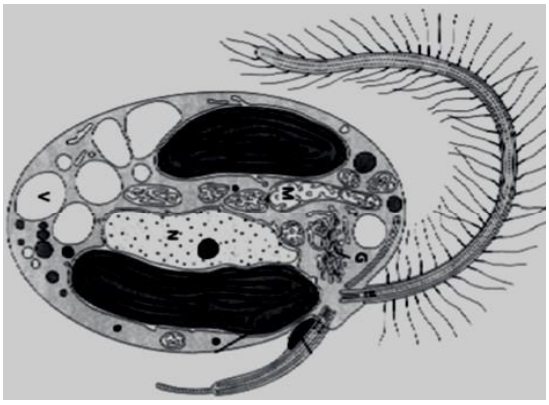

Figure 4.12: (a) Image of genus algae *ochrophyte* bearing mastigonemes on flagella[4]

Researchers utilize bio-inspired approach to designed artificial mastigonemes bearing flagella. A very few computational and experimental study is performed till date on mastigonemes and presented in this section.

From 2011 to 2018, computational study has been performed on mastigonemes bearing flagella for fluid mixing and pumping of fluid application. Namdeo et al. [4] stated that flagellum and mastigonemes shows independent and counteractive motion to each other. Flagellar and cilia motion is explored widely in literature while flagellar motion bearing mastigonemes is not studied much theoretically and experimentally. In 2013, Tottori and Nelson [31] in their work, first time fabricated the mastigonemes using three dimensional lithography to form ferromagnetic thin film using electron beam evaporation. A rotational motion is given to fabricated helical tail bearing mastigonemes through magnetic field. Work carried out towards study of mastigonemes flagella computationally and experimentally to date is summarized in Table 4.3.

Table 4.3: Work done to study flagella bearing mastigonemes

Year/Author	Design Parameters	Outcomes
1964- Jahn et al. [26]	Flagella L=1-1.3μm, D=15μm	In electron micrographs, the mastigonemes of *chrysomonads* seem to be rigid and presented at an average angle of 90°.
1967- Holwill and Sleigh [32]	Flagella L=19.8μm, D=0.25μm, No of mastigonemes per micron of flagella length 6.4, Length of mastigonemes-1.1μm,diameter-0.02μm	Water velocity-64.5μm/s is observed in the presence of *Ochromonas*. Swimming speed-55 μm/s to 60μm/s. If mastigonemes are present closely to each other and are more flexible as in case of *Euglena*, less fluid velocity is observed in comparison with uniformly distributed mastigonemes approximately 10-20% if mastigonemes are in a group of three.
1971- Bouck [25]	Fibrous Mastigonemes L=1-3 μm and D=50-100A°. Tubular L=1 μm and D-200A°	A flash photographs of the long flagellum shows that wave propagation is planar not helical. Studied structure, assembly and compositions of mastigonemes.
1975- Brennen [33]	EI=4×1016dynes cm2 and E= 5 dynes/μm2. Viscosity-10×10-10 dynes sec/ μm2. I=8×10-9 μm4	Ratio of velocity of propulsion for angle 10°, 20° and 30° to velocity of propulsion when mastigonemes are normal becomes 0.87, 0.76 and 0.56. Predicted propulsive velocity 60 μm/s matches well with the observed velocity 55-60 μm /s.
1996- Nakamura et al. [29]	Planar (Non-tubular mastigonemes- of Live cells of Chlamydomonas)	mAb-MAST1 increases the beating frequency of flagella and decreases the swimming velocity. This is the first direct evidence that mastigonemes play a role in motility, probably by increasing the effective surface area of flagella, and enhancing their propulsive force.
1996- Cahill et al. [28]	Tubular Mastigonemes (Zoospores)	Transmission electron microscopy of shadow cast, glutaraldehyde-fixed zoospores showed that the anterior flagellum of *P. cinnamomi* possesses two rows of mastigonemes. The mastigonemes are equally spaced along opposite sides of the flagellum and are perpendicular to the flagellar surface. The speed and velocity of movement, calculated from video recordings, were

Year/Author	Design Parameters	Outcomes
		218 and 294 μm/s, respectively
2009- Kobayashi et al. [34]	Flagella L=640μm, Quadrate (dxd,d=10μm). Mastigoneme: Height:0-100μm, width 5μm and depth: 10, 100μm. Number of mastigonemes:0-15	Examined the effect of number and dimensions of mastigonemes on thrust force and fluid flow using CFD.
2011-2018- Namdeo et al. [4]		CFD Study on mastigonemes flagella is performed; velocity of fluid is observed 1.5 mm/s. The mastigonemes project rigidly from the flagellar surface and interact with the surrounding fluid
2013- Tottori & Nelson [31]	Helical/Ferromagnetic thin film (Ni/Ti)/Water	Designed the length/spacing ratios of mastigonemes of α/β (a) 1/6, (b) 1/3, (c) 1/2, and (d) 1, at the constant a L/6, where L is the filament length of a one-turn helix. Other design parameters are selected as radius=5μm, angle 45°, number of mastigonemes=3, and α=0.7 μm. Experimentally and theoretically studied the critical length/spacing ratio where the reversal of motion occurs. The velocity slope becomes negative at α/β =1. This result shows that the mastigonemes structures generate a propulsive force opposite to the force generated by the main helical filament because hydrodynamic interaction take place between adjacent mastigonemes.

In the following sections, we first investigate the propulsive force enhancement by varying the number of branches keeping fluid medium and speed of the motor rotation constant. Then, orientation of branches on flagella and spacing between two consecutive branches is also compared to check their effect on propulsive force. In last, Taguchi analysis using Design of experiment (DOE) is applied to study the contribution of other factors in propulsive force measurement of branched flagellated swimmer.

4.4 Experimental Investigation of Branched Flagella

In engineering field, the most important movement of bio-organism is modelled to study its propulsive characteristics. In literature, shape, position and distribution of mastigonemes on *ochromonas* has been studied and its purification and isolation method

was developed. Planar motion of *ochromonas* was observed by high speed cinematography films. It has been noticed through simulation that when angle of mastigonemes changes from straight position (at 90°) to at an angle either towards head or away from head of *ochromonas* there is a decrease in propulsive velocity as mentioned in Table 4.3 by Brennen [33]. Scientists of various disciplines are making efforts in designing, modelling and controlling of bio-inspired flagella swimming of micro-organisms. A dimensional analysis of branched flagella has been done in Chapter 3 and investigation of dimensional parameters of branched flagella will be performed in the present chapter. The propulsive force of branched flagellated swimmer depends on the parameters listed below:

1. A flagellum having mastigonemes entails three important parameters as illustrated in Figure 4.13 (b) such as
   - Number of branches (mastigonemes) n,
   - Orientation of branches θ and
   - Spacing between branches S on flagella surface
   - System parameters such as speed of motor ω and effect of different viscosity of fluid medium is not studied yet at scaled up level experimentally.
2. Biocompatible material is the major concern in today's world for fabricating devices for biological applications. This study gives insightful observation on propulsive force generation by varying design parameters of branched flagella made up of biocompatible PDMS for its future biomedical applications.
3. The rigidity of branches is mentioned by EI, where E is the Young's modulus of elasticity and I is the moment of inertia.

In the following section, we keep length of flagella L, diameter of flagella D, length of branches ℓ, diameter of branches d and spacing between branches S constant and number of branches are varying on flagella to study the effect of propulsive force of flagella.

4.4.1 Effect of number of branches

Locomotion of bacteria in fluid at small scale is accomplished by cilia and flagella present on its surface. Enhancement in propulsive force through different designs of macro scale flagellated nanoswimmer is the main objective of the current research. In nature *ochromonas malhamensis* bears vertical appendages (mastigonemes) on flagella that locomote along with flagella in same direction and thrust force is mostly dominated

by mastigonemes [35], [29]. Till now working principle of flagella and cilia is utilized to design artificial microswimmer [36]-[37] for fluid flow and mixing of fluid at micron level while flagella bearing mastigonemes (Figure 4.13(a)) is not studied much in terms of propulsive characteristics [38]-[39]. In the vast literature, researchers have worked on non-branched flagellum (constant diameter flagellum and tapered flagellum) but effect of branches (i.e. mastigonemes) is not much attempted experimentally as well as analytically. Experiments are conducted at scaled up dimensions to show propulsive force enhancement due to mastigonemes using biocompatible material PDMS by mimicking mastigonemes on flagella. Consequently swimming velocity of the flagellated swimmer is zero and only reaction induced due to propulsive force is measured.

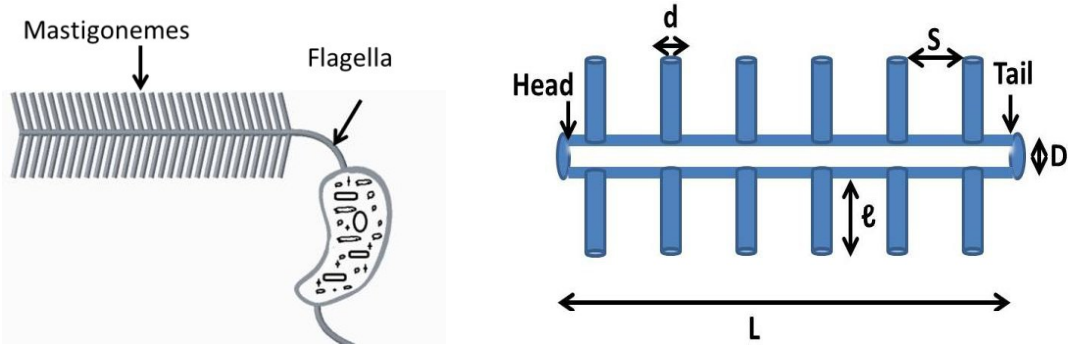

(a) (b)

Figure 4.13: (a) image of genus algae *Ochromonas malhamensis* [4] and (b) illustration of proposed design of flagella having mastigonemes. *L* and *D* are the length and diameter of flagellum whereas ℓ and *d* are length and diameter of mastigonemes (branches) and *S* is the spacing between two consecutive branches

Mastigonemes are considered as normal (at 90° orientation) on the surface of flagella in the present work. The main flagellum is defined by length and diameter as depicted in Figure 4.13(b). Schematic diagrams of three designs of flagella are considered by varying number of branches (Fig. 4.14(a)-(c)). The cylindrical cross section branched flagellated swimmer of length L and diameter D is covered by finite number of branches from 8, 16 and 24 in number towards distal end of flagella with uniform spacing S between branches. Branches are also taken as cylindrical cross section with uniform dimensions means length ℓ, diameter d and spacing S between branches throughout the length of flagella shown in Figure 4.13(b). Proximal end is considered as head and distal end is performing as tail end of branched flagella as shown in Figure 4.14(a) design.

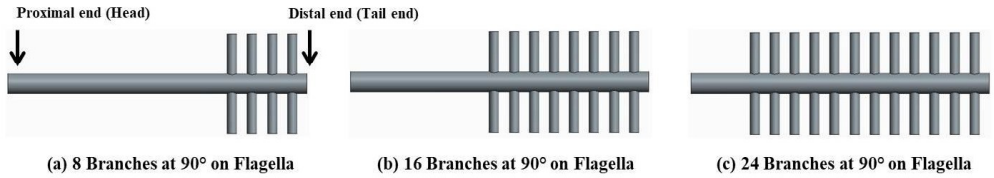

Figure 4.14: Designs (a)-(c) are having branches at 90°

PDMS biocompatible material is used to fabricate the branched flagella and is defined by Poisson's ratio (υ) 0.49 and Young's modulus (E) 2.46 MPa. Moulds for different designs are fabricated from aluminium material of prescribed dimensions (Table 4.4). PDMS polymer is mixed with curing agent in ratio of 10:1 and poured into moulds. The sealed mould is placed into oven at temperature 125°C for 20 minutes as mentioned in Chapter 3. After cooling the PDMS branched flagella is peeled off from mould. PDMS branched flagellated swimmer is immersed in high viscosity 350 cSt silicon oil to maintain the low Reynolds numbers environment experienced by micro-organisms in nature. The size of the system design is scaled up to manageable level. The geometric parameters are scaled up to simplify the fabrication and actuation, using Buckingham dimensional analysis and experiments are carried out in highly viscous silicon oil. The dimensions of the branched flagella are scaled up 3000 times to the dimensions, to mimic biological bacteria and also to make easier the fabrication procedure as discussed in Chapter 3. The geometric parameters are chosen for branched flagellated swimmeris in Table 4.4.

Table 4.4 Dimensional parameters of branched flagellated swimmer

Design Parameters	**Length (mm)**	**Diameter (mm)**
Flagella (*L*, *D*)	150	10
Branches (ℓ,*d*)	20	5

Due to prescribed rotation ω 100 RPM, macro-swimmer swims in forward and backward direction with net propulsion velocity at one end of flagella (head) through scotch yoke mechanism. The flagellated swimmer undulates in a stationary tank (300 mm × 200 mm × 200 mm) filled with silicon oil. As head is constrained to move in y direction due to flagella undulation, swimming speed remains zero and propulsive force is measured in z direction. Figure 4.15 shows the schematic diagram and actual

experimental set up consists of DC motor and rotation of motor was converted into planar oscillation via scotch yoke mechanism. DC motor (placed on cantilever beam) is switched on branched flagella oscillate in *y* direction inside the silicon oil filled chamber and generate the deflection in *z* direction of cantilever beam. The cantilever beam deflection is measured using Laser Micrometer and converted into thrust force by equation (4.1).

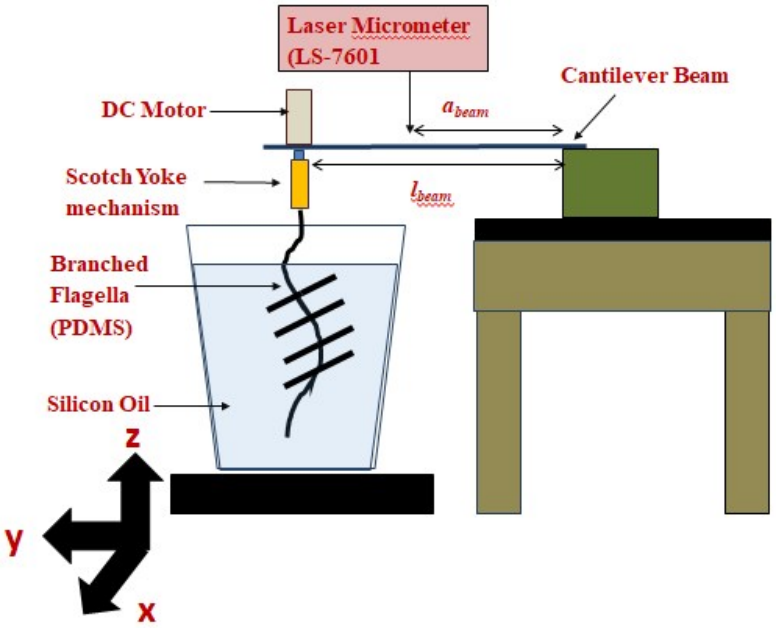

(a)

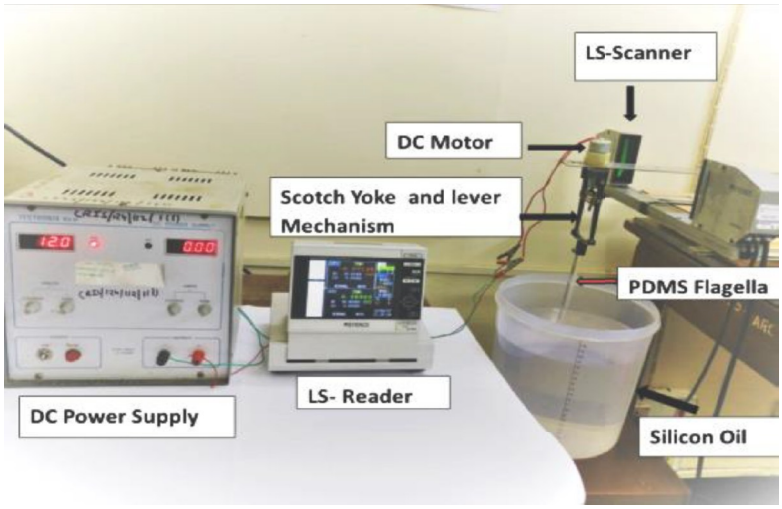

(b)

Figure 4.15: (a) and (b) schematic and experimental set up of scaled up level, for branched flagellated swimmer

PDMS branched flagella is coupled with DC motor using scotch yoke mechanism. The motor flagella assembly is mounted on an aluminium cantilever beam which is 300 mm long. The cross section of beam is rectangular with 50 mm by 1.86 mm shown in Appendix I. Deflection of cantilever beam generated due to planar motion of branched flagella is measured through Keyence laser micrometer LS-7601, placed at distant a_{beam} away from DC motor.

The relation between propulsive force generated and cantilever beam deflection is given by equation (4.1):

$$\text{Propulsive Force: } F = \frac{\delta_{beam} \times E_{beam} \times I_{beam}}{\left[\frac{(l_{beam} - a_{beam})^3}{6} + \frac{l_{beam}^2 \times a_{beam}}{2} - \frac{l_{beam}^3}{6}\right]} \quad (4.1)$$

where, F is the propulsive force, δ_{beam} is the deflection of beam, E_{beam} is the young's modulus elasticity of aluminium cantilever beam (69 GPa), I_{beam} is the moment of inertia of cantilever beam (2.21 mm^4), l_{beam} is the length of beam (300 mm) and a_{beam} is the distance (135 mm) at which deflection of cantilever beam is measured through laser micro-meter.

Designs of fabricated PDMS branched flagella are depicted in Figure 4.16. The length and diameter of flagella is same in all the designs. The number of branches is varied keeping space between branches constant. The branches are taken symmetrical on both sides of flagella. The experiments are performed on 8, 16 and 24 branches flagella (Figure 4.16(a-c)). The experiments are conducted in silicon oil medium having viscosity 350 cSt and motor speed is kept 100 RPM to maintain low Reynolds number (Re≈1) regime. Data of deflection of cantilever beam is recorded for time duration of 256 sec through Keyence laser micro-meter.

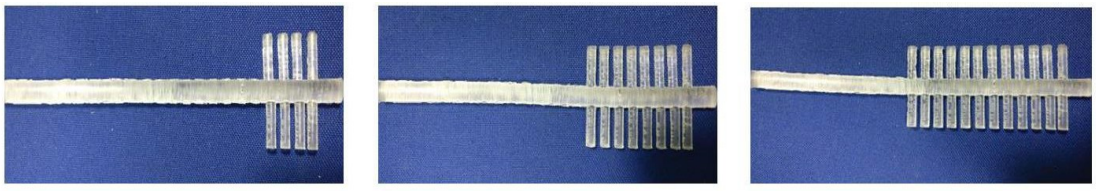

(a) 8 Branches at 90° on Flagella (b) 16 Branches at 90° on Flagella (c) 24 Branches at 90° on Flagella

Figure 4.16: Showing designs of PDMS fabricated branched flagella

4.4.2 Results and discussion

Whenever experimentation instigated each time, laser micrometre is switched on and then zeroed. The flagellum is run at 100 RPM for several minutes to attain steady state after that data acquisition is initiated. After each run the laser micro-meter is reset and test begin again. Figure 4.17 shows the response of deflection of cantilever beam in terms of propulsive force due to planar motion of flagellated swimmer where laser scanner is placed. The effect of branches in terms of deflection of cantilever beam is recorded through laser reader. The recorded deflection data for each design of branched flagellated swimmer is recorded and respectively propulsive force is calculated using equation (4.1) and plotted on *y*-axis as shown in Figure 4.17(a). As number of branches increases from 8 to 24 towards proximal end of flagella, the deflection of cantilever beam also increases. Maximum deflection is observed for 24 branched flagella is 0.051 mm. Propulsive force calculated for 24 branched flagella is 3.34±0.015 mN and mentioned in Figure 4.17(a), which is approximately in the range of propulsive force 6 μN to 80 mN as reported in literature [17]-[22] and mentioned in Table 4.2. Though dimensions used are not same and experiments are conducted on non-branched flagella. In experimental study the signal is picked up through laser micro-meter from deflecting cantilever beam due to head movement of flagella attached to DC motor inside the silicon fluidic chamber. Cantilever beam is used as a deflection sensor. The results are leading towards possible design by improving the propulsive force of branched flagella. Each branched flagella has uniform diameter throughout the length and is made up of linearly elastic, biocompatible PDMS material.

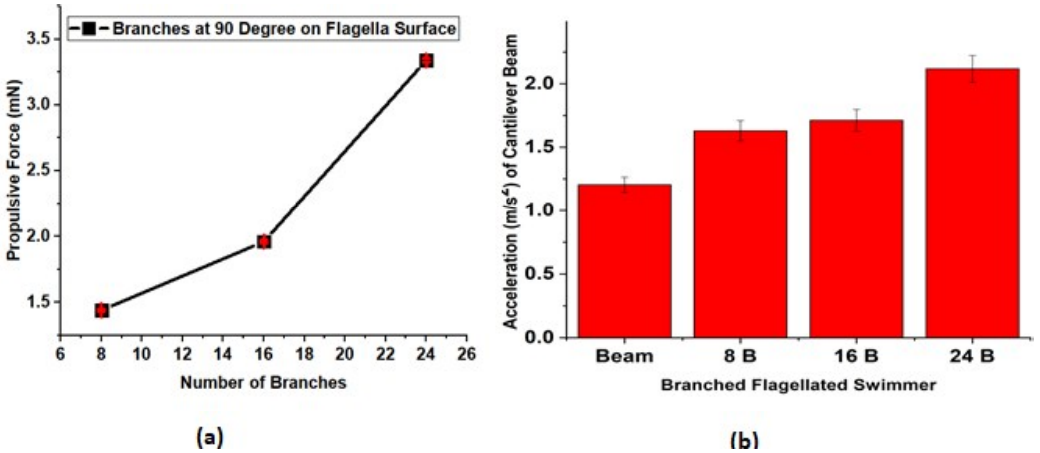

Figure 4.17: (a) Plot of propulsive force measured experimentally with respect to number of branches and (b) plot of RMS value of FFT for different branched flagella

The branched flagellated swimmers are fabricated to experimentally quantify propulsive force engendered through planar mode of propulsion. Experimentation is being performed with 90° oriented branched flagella to validate the trend of increment in propulsive characteristics by adding number of branches respectively at 100 RPM speed of DC motor. To corroborate the effects of increase in number of branches, we have fixed accelerometer a type of vibration sensor on cantilever beam to measure driving acceleration level and recorded the Fast Fourier transform (FFT) data for each designed branched flagellated swimmer. Vibration sensor also called as accelerometer is shown in Figure 4.18 and used in the experimental investigation to show substantiality of the branches on flagella. In case of random vibration, a power spectral density is taken in consideration while for sinusoidal vibration of cantilever beam provided by scotch yoke mechanism acceleration is being taken as analysis part. A root mean square (RMS) value for each FFT data is observed in Fig. 4.17(B) for cantilever beam without branched flagella and with branched flagellated swimmer. RMS is used for calculating the strength of signal wave. It is found that there is an increase in RMS value from FFT of cantilever beam without flagella to the FFT RMS of cantilever beam with branched flagellated swimmer. There is an increase in 23% RMS value of FFT data on increasing number of branches from 8 to 24. RMS value observed for 24 branched flagella is 2.12 ± 0.11 ms^{-2}. FFT data with their RMS value for 8, 16 and 24 branched flagella is shown in Figure 4.17(B).

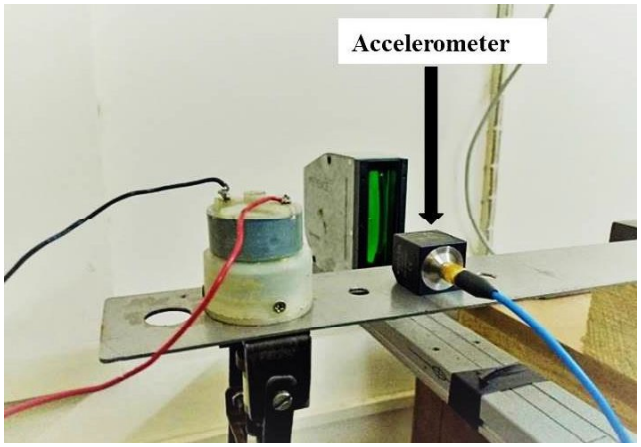

(a)

Figure 4.18 shows placement of accelerometer on cantilever beam for recording FFT data

4.4.3 Comparison of 60°, 90°, 120° oriented branched flagella

In literature, it is mentioned that when mastigonemes moves in forward and backward direction along with flagella it bends at an angle other than 90°. Researchers have hydro-dynamically simulated and evaluated the propulsive velocity of mastigonemes as mentioned in Table 4.3. Here, we carry out the experimental investigation branches on flagella at angle 60°, 90°, 120°. Moulds are designed and PDMS 24 branched flagella (because providing enhanced propulsive force) is fabricated for orientation of branches 60°, 90°, 120° shown in Figure 4.19(a), (b) and (c).

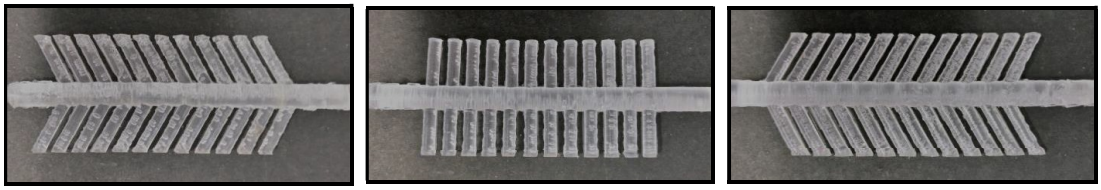

(a) (b) (c)

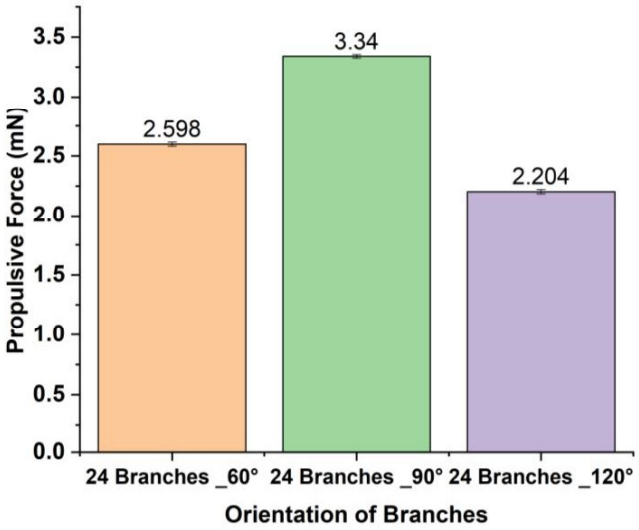

Figure 4.19: 24 branches at (a) 60°, (b) 90°, (c) 120° on flagella surface and (d) comparison of propulsive force of branched flagella

The dimensions of 24 branched flagella shown in Figure 4.19 are same as mentioned in Table 4.4 for all three designs only orientation of branches are changed as 60°, 90° and 120°. The experiments are done on planar actuation of 24 branched flagella at 100 RPM immersed in silicon oil medium (350 cSt). The deflection of cantilever beam is obtained through laser micro-meter and propulsive force is calculated using equation (4.1). All the experimental studies are performed at same environmental condition. Laser micro-meter is on and deflection of cantilever beam due to planar motion of 24 branched flagella is recorded for

256 seconds. The recorded deflection is used for calculating propulsive force and plotted as graph shown in Figure 4.19 (d). The maximum propulsive force 3.34±0.015mN is observed for branches at 90° orientation on flagella while 60° and 120° oriented 24 branches shows 2.59±0.0167 mN and 2.20±0.0174 mN propulsive forces. The propulsive force ratio for 60° and 120°oriented branches decreases to 0.77 and 0.66 with respect to propulsive force calculated for 90° oriented 24 branched flagella. The experimental results clearly show the significance of 90° oriented branched flagella. In the next section study of propulsive force generated, on varying the spacing between branches over the length of flagella are performed.

4.4.4 Variation of spacing between 8 branches flagella oriented at 90°

Here, the experimental exploration is carried out to investigate how the increase in spacing between branches affects the propulsive force. The two designs of 8 branches flagella are studied through experimental analysis. The results are interpreted in terms of the propulsive force generated at the head of branched flagella attached to the scotch yoke mechanism for planar propulsion. In the current study, uniform dimensions of branches are considered over the length of flagella. The dimensions of the fabricated branched flagella are scaled up with approximately 3000 times of the paramecium to make easier the fabrication procedure and to maintain low Reynolds number regime. The geometric parameters chosen for fabrication of 8 branched flagellated swimmer; the dimensions of branches are length l 20 mm and diameter d 5 mm and dimensions of flagella are length L 150 mm and diameter D 10 mm at scaled up level same as given in Table 4.4. A scotch yoke mechanism translates rotational motion into linear motion to engender planar wave movement of attached flagella. The cantilever beam is deflected due to thrust force generated by planar motion of branched flagella in viscous medium which is measured by Keyence LS-7601 laser micro-meter. The schematic of experimental set up for nanoswimmer is shown in Figure 4.26(b).

Both designs of nanoswimmer as depicted in Figure 4.20; have same length and diameter for flagella as well as 8 number of branches are also same and spacing S between branches are getting changed. The branches (mastigonemes) are taken symmetrical on both sides of flagella. In Figure 4.20(a) the spacing S between branches are of 3 mm while in Figure 4.20(b) the spacing between branches are 11 mm ($2S+d$, where d is the diameter of branch). The 8 branched flagella is chosen because of limited length of

flagella available for both case of spacing *S* and 2*S*+*d* between two consecutive branches. If 24 branch flagella is used for study, it is not possible to accommodate 24 branches on flagella with spacing 2*S*+*d*. The experimental study is performed for propulsive force generation due to the oscillatory motion of 8 branched flagella structure for comparison. The angle of branches is at 90° orientation for both the case as shown in Figure 4.20. For design (a) and (b) (Figure 4.20) propulsive force value is approximately 1.44±0.02 mN and 1.58±0.015mN as shown in Figure 4.20(c). In bar graph, *x*-axis represents the 8 branches flagella with different spacing and *y*-axis represents the propulsive force generated due to planar motion of each designs of 8 branch flagella. The percentage increase in propulsive force is observed as 9.72%. Both the designs of 8 branch flagella are fabricated from PDMS by standard procedure given in detail in Chapter 3. The experiments are conducted at 100 RPM rotation of DC motor connected to scotch yoke mechanism and silicon oil of 350 cSt is used as fluidic medium to maintain low Reynolds number.

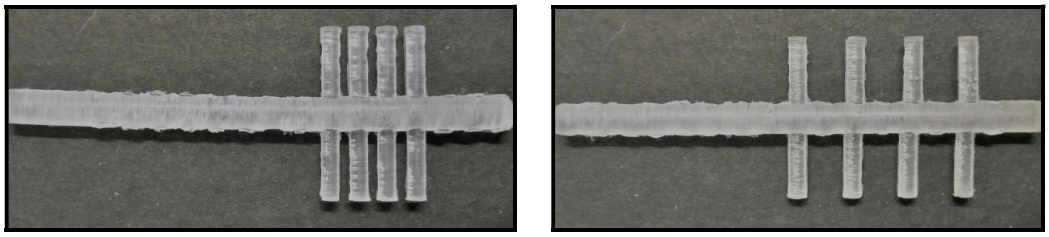

(a) (b)

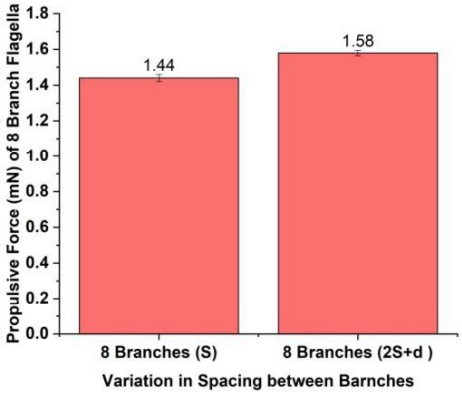

(c)

Figure 4.20: (a) and (b) show 8 branch flagella with spacing *S and 2S+d* and (c) shows the percentage increment in propulsive force by varying the spacing between 8 branch flagella

4.5 Parametric Study for Locomotion of Branched Flagella

In the above section, increase in number of branches and spacing between two consecutive branches are assumed and found to enhance propulsive force at 90° orientation of branches on flagella surface as discussed in section 4.4. Number of branches is increased from 8, 16 and 24 in number and system parameters such as viscosity of medium and speed of motor is chosen same in all the experimental studies. Now, we need to study the contribution of the environmental parameters like speed of motor and viscosity of medium for the designed test rig to locomote branched flagellated swimmer. Finally, our quantitative and statistical analysis of enhanced propulsive force due to planar motion of branched flagellated swimmer highlights the potential of number of branches, angle of branches and spacing between branches on flagella surface along with environmental parameters. The prototype fabrication does not require any specialization and thus quick, low cost technique and facilitate the production of branches on flagella at different angle, varying number of branches and spacing between branches on flagella surface. The subsequent section presents the Taguchi optimization technique to study the impact of speed of DC motor, viscosity of medium and number of branches on the propulsive force generation due to branched flagellated artificial swimmer. Orthogonal array (OA), Signal to Noise ratio (S/N) and Pareto analysis of variance (ANOVA) are applied to examine the effect of environmental parameters as well as design parameters of flagella on locomotion of branched flagella.

4.5.1 Taguchi analysis: design of experiments (DOE)

Two key parameters used in Taguchi analysis to optimize design for its better performance and qualities are: orthogonal array which acclimatize several design factors simultaneously and Signal to Noise (S/N) ratio which deals with quality due to variation. Taguchi method lessens the time required for experimental analysis and helps to explore the effect of different factors as well as to study which parameter has more impact and which has less effect on the outcome of analysis. The present study describes a case study on branched flagellated artificial swimmer. The aim is to find a combination to achieve maximum propulsive force.

Process for doing experiments design incorporate following steps:

1. Write down the control parameter and noise factor of the procedure.
2. Find out the level of each parameter. Then, select orthogonal array (OA).
3. Perform experiments as per selected OA.
4. Calculate S/N ratio from the experimental data.
5. Analyze the result by performing S/N ratio to check the main effect of parameter and by applying Pareto ANOVA to see the contribution of each factor.

In the past, Taguchi has been employed for manufacturing process development and now days it is being used by engineers, biologist, and mathematician and so on for their application area. Control factors are taken such that effect of noise factor has been abolished.

The most important point in the design of an experiment stays in the selection of control factors. The S/N ratio is used to measure the quality of the product and takes into consideration both mean and variance and also consider the level of performance effect of environmental disturbance factor to study the output characteristics. The S/N ratio is used for two applications; first is enhancement in measurement and another is quality improvement by decreasing the variation. The S/N ratio can be categorized as:

Normal is the better characteristics: $$S/N = 10\log\frac{x_{\text{average}}}{X_{\text{variance}}} \quad (4.2)$$

Larger is the better characteristics: $$S/N = -10\log\frac{1}{n}\sum\frac{1}{x^2} \quad (4.3)$$

Smaller is the better characteristic: $$S/N = -10\log\frac{1}{n}\sum x^2 \quad (4.4)$$

where, x is the observed data and n is the number of observations. For every type of S/N ratio characteristics, larger the value better is the result. Conventional methods of design of experiments required a large number of experiments with increase in number of parameters and its levels. S/N ratio measures the both rank of performance and influence of noise factors on performance of output characteristics. In the present work we have investigated the maximum propulsive force as performance index and have chosen larger-the-better S/N ratio.

4.5.2 Experimental investigation of branched flagella: DOE

The design of experiment is approach of experimentation through which complete information of experimental system can be achieved by doing minimum trials. Experimental design has several advantages. It helps in recognizing the important process parameter, which will control and improves the process. It also helps in the development of the new methods for which historical data are not available. In a standard methodology, one factor is kept constant and other factors are varying at a time. This approach may not be useful if the interaction between the factors is present. To study the interaction between factors, a full factorial design is used but it leads to more number of experiments which is not possible practically sometime and it is also time consuming. So, DOE seems more promising methodology through which less number of experiments can be done to study the interaction between different parameters and levels. However the technique is well developed and used in various engineering applications but is not reported in the field of flagellated artificial swimmer. The present study is an effort to scrutinize the effect of various designs of artificial branched flagellated swimmer and its environmental factors. The influence of speed of motor, viscosity of medium and effect of branches on the propulsive force generation of branched flagella is investigated experimentally through DOE. The Taguchi's statistical method is used to design the experiments and hierarchical levels are drawn to conclude a most significant parameter, which can alter the propulsive force value of various designs of branched flagella.

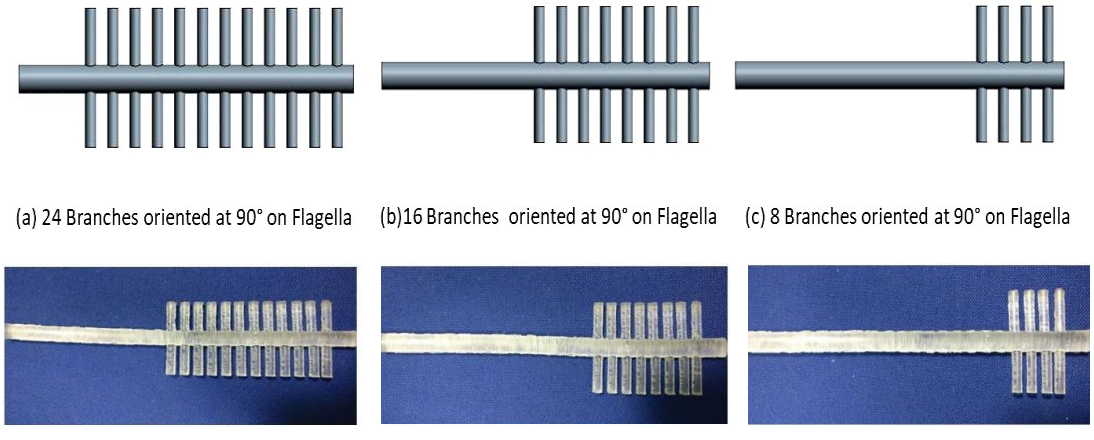

Figure 4.21: Branches at 90° orientation on flagellated swimmer

In DOE, the essential step is the selection of control factors. The control factors are included as many as possible to recognize the insignificant variable at the early stage of the experimental studies. Major parameters which influence the propulsive forces are; 1) speed of motor; 2) viscosity of fluid medium and; 3) number of branches. Here, we study the DOE for 8, 16 and 24 branches designs of flagellated swimmer shown in Figure 4.21. With three parameters as variables and considering three levels of each variable, a fractional factorial design of 3^3 experiments are done with L_9 orthogonal array. The orthogonal array has potential to check the relation between different parameters. Table 4.5 shows the 3 control parameters and their levels. Three levels are represented by a '1' or a '2' or a '3' shown in Table 4.6. Three parameters are arranged in 1-4 columns in the standard L_9 orthogonal array as shown in Table 4.6. In table 4.6, A, B, and C is used as notations and represents the speed of DC motor, viscosity of silicon oil medium and number of branches on flagella surface. The parametric values used for speed of DC motor and silicon oil medium is chosen to maintain low Reynolds regime in conducting scaled up experiments. The experimental analysis is carried out at room temperature under specified environmental conditions and with expertise in handling experimental system while recording the resulting data of deflection of cantilever beam from laser micro-meter. The deflection of cantilever beam is converted into propulsive force and studied for S/N ratio analysis. The objective of experiment is to optimize the parameters for better propulsive force and larger the better characteristics is used. Table 4.7 shows the computed S/N ratio for resulting propulsive force through mini-tab software.

Table 4.5: Control parameters and their levels

Parameters	**Level 1**	**Level 2**	**Level 3**
Speed of DC motor (RPM)	200	300	500
Viscosity of silicon oil medium (cSt)	10000	15000	20000
Number of branches	24	16	8

Table 4.6: The basic Taguchi L_9 orthogonal array

Experiments	A	B	C	Notation
1	1	1	1	$A_1B_1C_1$
2	1	2	2	$A_1B_2C_2$
3	1	3	3	$A_1B_3C_3$
4	2	1	2	$A_2B_1C_2$
5	2	2	3	$A_2B_2C_3$
6	2	3	1	$A_2B_3C_1$
7	3	1	3	$A_3B_1C_3$
8	3	2	1	$A_3B_2C_1$
9	3	3	2	$A_3B_3C_2$

Table 4.7: S/N ratio for propulsive force response of 90° oriented branched flagella

Experiments	Speed of DC motor (RPM)	Viscosity (cSt)	Number of Branches	S/N ratio of 90° oriented branched Flagella
1	200	10000	24	8.7788
2	200	15000	16	4.1335
3	200	20000	8	3.1371
4	300	10000	16	5.6990
5	300	15000	8	4.7786
6	300	20000	24	13.9424
7	500	10000	8	4.4940
8	500	15000	24	10.1166
9	500	20000	16	16.4256

4.5.3 Parametric optimization of branched flagellated swimmer

The aim of experimental investigation is to optimize the branched flagellated swimmer designs and its environmental conditions to get better propulsive force; the larger the better characteristics are used. Whereas Table 4.7 shows the mean S/N ratio for each level of propulsive force of 90° oriented branched flagella shown in Figure 4.21 to

investigate initially the behaviour of each experiments conducted at scaled up level and their corresponding S/N ratio for L_9 standard orthogonal array. The data represented in Table 4.7 is then plotted in Figure 4.22. The propulsive force attained for each set of trials of nine experiments has been subjected to statistical analysis. The DOE is utilized to enhance the parametric value for advancement of results. Standard experimental process is generally lengthy, complex and not always fulfils the desired purpose. The average S/N ratios for all three parameters for all levels presented in Table 4.7 are plotted and shown in Figure 4.22 for 90° oriented branched flagellated swimmer. From Table 4.8, it is clear that branches are one of the most significant parameter, which influences the propulsive force. The other parameters namely speed of motor and viscosity of silicon oil medium follows in this order to influence the deflection of cantilever beam resulted in propulsive force of branched flagella.

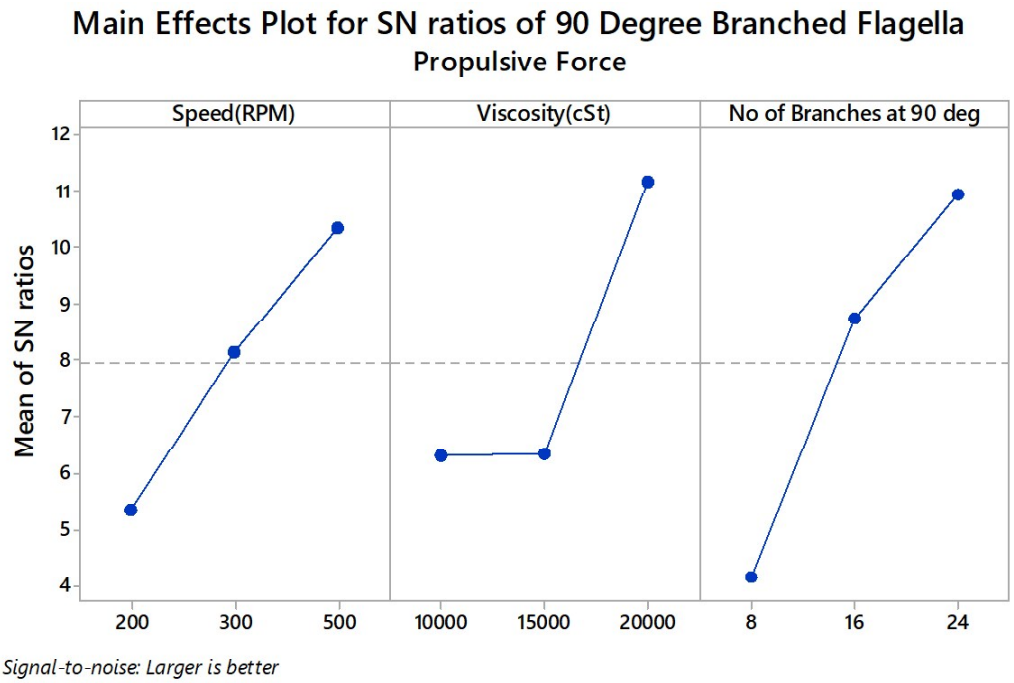

Figure 4.22: The larger the better signal graph for 90°oriented branched flagellated swimmer through experimental investigation

From Figure 4.22, it is clear that the level 3 of parameter C will cause the highest deflection value and hence more number of branches will be the best choice to have higher deflection of cantilever beam. Similarly, for the second more influencing parameter that is speed of motor (parameter A) level 3 is more influencing. Viscosity of

fluid medium (parameter B) is the third parameter with level 3 is suitable. Therefore, the best combination of the experimental set is $A_3B_3C_3$. Table 4.8 shows the best value of each factor and its level. As the experiment of the combination $A_3B_3C_3$ was not performed in the set of 9 experiments. The difference between the levels of each factor denotes the influence of the affect. Larger is the difference, stronger the influence.

Table 4.8: Response table for average S/N ratio for propulsive force of 90° oriented branched flagella

	S/N for Speed of Motor	S/N for Viscosity of Fluid Medium	S/N for 90° Oriented Branch Flagella
1	5.350	6.324	4.137
2	8.140	6.343	8.753
3	10.345	11.168	10.946
Max-Min	4.996	4.844	6.809
Rank	**2**	**3**	**1**

Table 4.9: Optimized value of factors and levels

Factors	**Optimized Value**
Speed of Motor (RPM)	500
Viscosity of medium (cSt)	20000
Number of Branches	24
Propulsive Force	7.25 mN

The analysis of results indicates that the optimized combination for high propulsive force is high speed of motor, high viscosity of medium and more number of branches. The best level of combination ($A_3B_3C_3$) at which experiments are performed further are speed of DC motor 500 RPM, viscosity of silicon oil fluidic medium 20000 cSt and 24 number of branches flagella and propulsive force are obtained as 7.25 mN.

Same trend of S/N ratio main effect plot is also observed for 60° and 120° oriented branched flagellated swimmer shown in Figure 4.23, by doing same Taguchi analysis as done above in the case of 90° oriented branched flagella. Table 4.10 shows S/N ratio

for both 60° and 120° oriented branch flagella. Graphs of mean S/N for both 60° and 120° oriented branch flagella is shown below in Figure 4.24. Table 4.11 and Table 4.12 show the response table for average S/N Ratio for propulsive force of 60° and 120° oriented branched flagella. The Rank of different parameters is given as number of branches is first order, speed of motor at second order and viscosity of medium at third place.

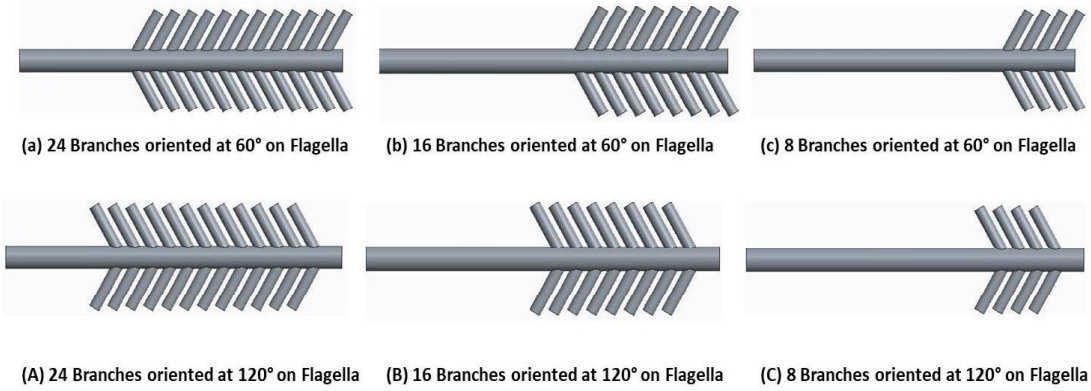

Figure 4.23: Showing branches orientation at 60° and 120° on flagella surface

Table 4.10: S/N ratio for propulsive force response of 60° and 120° oriented branched flagella

Experiments	Speed of DC motor (RPM)	Viscosity (cSt)	Placement of Branches	S/N ratio of 60° oriented branched Flagella	S/N ratio of 120° oriented branched Flagella
1	200	10000	24	6.27092	5.99352
2	200	15000	16	3.36413	2.62815
3	200	20000	8	2.10727	1.68963
4	300	10000	16	5.62727	5.34794
5	300	15000	8	3.35326	2.87855
6	300	20000	24	8.13611	7.76314
7	500	10000	8	4.33488	3.62085
8	500	15000	24	7.59040	7.00172
9	500	20000	16	9.97122	9.37498

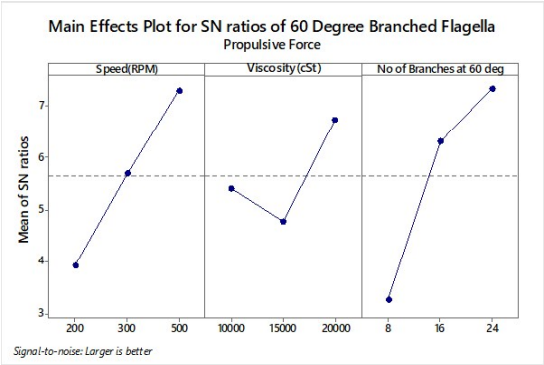

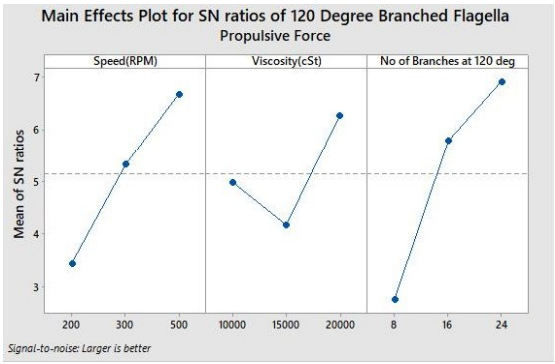

(a) (b)

Figure 4.24: (a) and (b) showing S/N ratio for 60° and 120° branched flagellated swimmer

Table 4.11: Response table for average S/N Ratio for propulsive force of 60° oriented branched flagella

	S/N for Speed	**S/N for Viscosity**	**S/N for Branches**
1	3.914	5.411	3.265
2	5.706	4.769	6.321
3	7.299	6.738	7.332
Max-Min	3.385	1.969	4.067
Rank	**2**	**3**	**1**

Table 4.12: Response table for average S/N ratio for propulsive force of 120° oriented branched flagella

	S/N for Speed	**S/N for Viscosity**	**S/N for Branches**
1	3.437	4.987	2.730
2	5.330	4.169	5.784
3	6.666	6.276	6.919
Max-Min	3.229	2.106	4.190
Rank	**2**	**3**	**1**

4.5.4 Pareto ANOVA analysis

Pareto ANOVA is one of the methods for optimization of process [40]. It is possible to evaluate the response magnitude in terms of percentage (%) of each parameter in the orthogonal experiments. Pareto ANOVA does not necessitate ANOVA, so no need of *F*-test. Pareto ANOVA use S/N ratio. From the results taken the best combination to get higher value of propulsive force is at level '3' of speed of DC motor, level '3' of viscosity of silicon oil fluid medium and level '3' of branches on flagella. It is observed form the result that in order to acquire more propulsive force always use higher level of speed of motor, viscosity of fluid medium and number of branches on flagella surface. For a given parameter and level, the square of the difference (SD) for each level is calculated and their sum is taken. The percentage contribution of each parameter is also evaluated by dividing each SD corresponds to each parameter by sum of SD. This method is quick and easy to analyse the results of parametric variation in an experiment without requirement of detailed ANOVA and *F*-test. Pareto ANOVA analysis does not require much awareness about ANOVA and appropriate for engineering application. The percentage contribution of each parameter is shown in Figure 4.25. From the results acquired as shown in Figure 4.25 for propulsive force, the contribution of number of branches are 46.22%, 53.63%, 47.77% for 90°, 60° and 120° oriented branches on flagella.

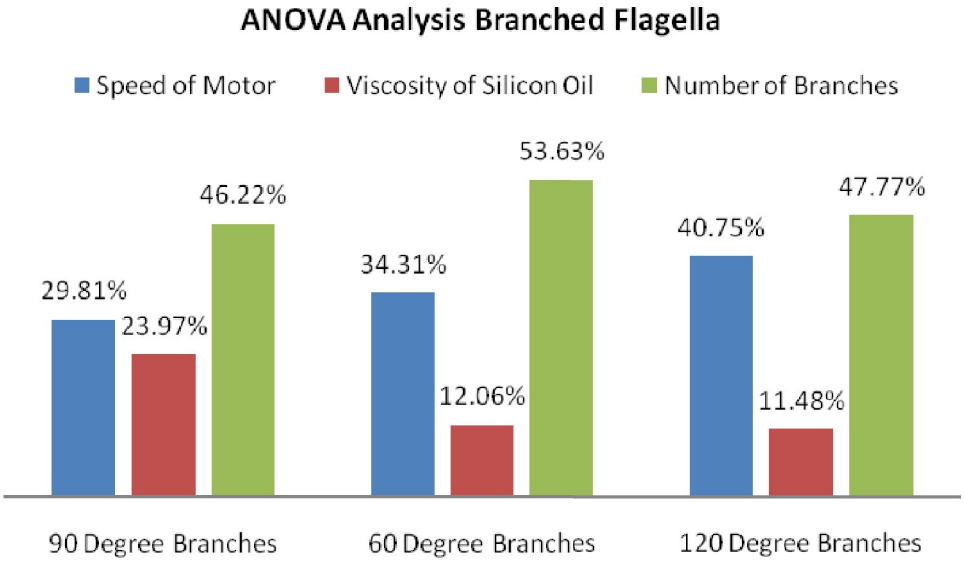

Figure 4.25: ANOVA analysis to show contribution percentage of each parameter

4.6 FEM Simulation of Branched Flagella: COMSOL Multiphysics

In this study, the effect of increase in number of branches of modelled branched flagellated swimmer on propulsive force is studied for further verification of experimental results. Mastigonemes (branches) are considered as normal on the surface of flagella which is considered as 90° in the present work shown in Figure 4.14. The main flagellum is defined by length and diameter as depicted in Figure4.13 (b). The cross section of branched flagellated swimmer of length L and diameter D is covered by finite number of branches from 8, 16 and 24 in number towards distal end of flagella with uniform spacing S between branches. Branches are also taken with uniform dimensions means length ℓ, diameter d and spacing S between branches are kept same throughout the length of flagella. Proximal end is considered as head and distal end is performing as tail end of branched flagellated swimmer as shown in Figure 4.13 (a) design. The flagellated model undulates in a stationary tank (300 mm × 200 mm × 200 mm) filled with silicon oil. As head is constrained to move in y direction due to flagella undulation, swimming speed remains zero and propulsive force is measured in z direction.

Fluid solid interaction module is considered to simulate branched flagellated swimmer. The analysis of the system model is done in COMSOL@5.4 software in which equation of laminar flow around branched flagella and solid mechanics module are coupled to simulate the flagella head displacement. At low Reynolds number, the laminar flow physics in COMSOL is governed by Stokes equation (4.2) for linear viscous incompressible fluid as shown;

$$-\nabla P + \mu \nabla^2 u = 0 \tag{4.2}$$

where, P is the pressure, μ is the fluid viscosity and u is the velocity of fluid. While in solid mechanics module, linear elastic material property is used which indicates that when designed model deforms it generates internal stresses because of prescribed loading condition. Linear elastic module consists of equation of motion (Newton's second law), strain-displacement equation and constitutive equation governed by Hooke's law given by equations (4.3), (4.4) and (4.5) respectively.

Equation of motion: $$\rho \frac{\partial^2 u_{solid}}{\partial t^2} = \nabla \sigma + F \tag{4.3}$$

Strain-displacement equation: $$\varepsilon = \frac{1}{2}\left[\nabla u_{solid} + (\nabla u_{solid})^T + \nabla u_{solid}(\nabla u_{solid})^T\right] \quad (4.4)$$

Constitutive equation: $$C = C(E, \upsilon) \quad (4.5)$$

where, u_{solid} is the displacement, ρ is the density of material, σ is the Cauchy stress tensor, F is the body force per unit volume, ε is the strain tensor, C is the stiffness tensor, E is the Young's modulus and υ is the Poisson's ratio. To investigate the effect of number of branches on flagella length, we define the planar beating on head i.e. proximal end of branched flagella swimmer, in positive y direction is defined with velocity v_y

$$v_y = A\omega \sin \omega t \quad (4.6)$$

where, A is the amplitude and ω is the frequency at which head of branched flagellated swimmer is beating. The results of COMSOL are analysed and interpreted in terms of propulsive characteristics of branched flagellated swimmer. The elastic properties of the macro swimmer flagella chosen corresponding to PDMS biocompatible material same as used in conducting experiments and are defined by Poisson's ratio (υ) 0.49 and Young's modulus (E) 2.46 MPa. Due to prescribed velocity v_y, macro-swimmer swims in forward and backward direction with net propulsion velocity at one end of flagella (head) in solid mechanics module. PDMS branched flagellated swimmer is immersed in high viscosity 20000 cSt silicon oil to maintain the low Reynolds numbers environment experienced by micro-organisms in nature. The dimensions of the modelled branched flagella are scaled up 3000 times to the dimensions, to mimic biological bacteria and also to make easier the fabrication procedure. The geometric parameters are chosen for branched flagellated swimmer is in Table 4.4.

Physics controlled mesh with element size normal is used to set mesh. It gets information from physics by which element domain and periodic condition is used automatically to provide suitable mesh sequence. The numbers of mesh elements are 32495. The mesh of the designed model is shown in Figure 4.26.

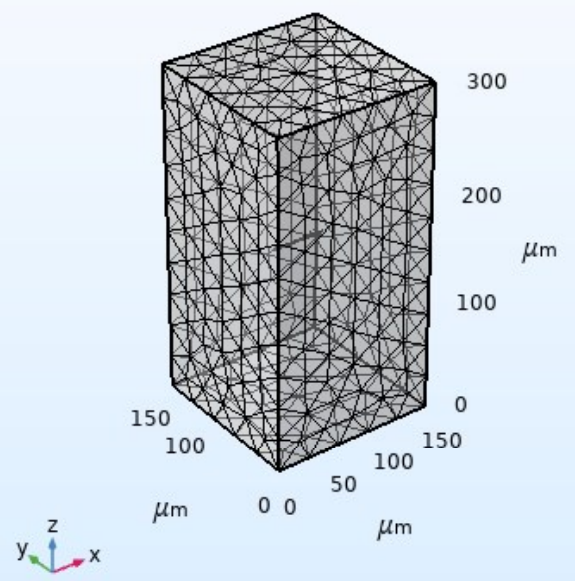

Figure 4.26: Meshed model of outer container consisting of PDMS based macroscale branched flagellated artificial nanoswimmer.

The displacement (mm) of proximal end of each design of branched flagellated swimmer shown in Figure 4.14 is plotted in Figure 4.27(A). The *x*-axis denotes the number of branches and *y*-axis shows the value of displacement occur for each design of branched flagellated swimmer at 90° of branch orientations. As number of branches increases from 8 to 24, displacement of head of flagella also increases from 9.39 mm to 9.89 mm for 90° branched flagella. Figure 4.27(A) shows that as number of branches increased from 8 to 24, increase in head deflection for 90° oriented branched flagellated swimmer is observed as 5.19%. In literature, it was mentioned that mastigonemes should be rigid enough for generating propulsive speed [36]. If modulus of elasticity of mastigonemes is less, performance of mastigonemes under applied load condition is not sufficient to increase the propulsive velocity. Here, PDMS biocompatible material is taken for modelling in COMSOL for analysis of variation of 90° oriented branch which is rigid enough to produce propulsive force.

In COMSOL simulation results, maximum head displacement is observed for 24 branches placed at 90° orientation with respect to flagella. In Figure 4.27(B), propulsive force of 8, 16 and 24 branched flagellated swimmers are shown along with propulsive force measured from experimental results. The experiments are performed on same simulated conditions such as number of branches are taken as 8, 16 and 24 at

90° orientation on flagella surface, speed of motor is set as 500 RPM and viscosity of silicon oil is chosen as 20000 cSt. There is a difference in propulsive force measurement for experimental results. Simulated propulsive force for 24 branched flagellated swimmer is 11.37 mN and experimental propulsive force is measured as 7.24 mN. In simulation we are directly measuring the propulsive force on head of flagella while in experiments the generated propulsive force is measured through cantilever beam deflection. The trend of graph plotted in Figure 4.27(C) and (D) is sinusoidally varying with respect to time when prescribed velocity is applied to the proximal end (head) and distal end (tail) of flagella

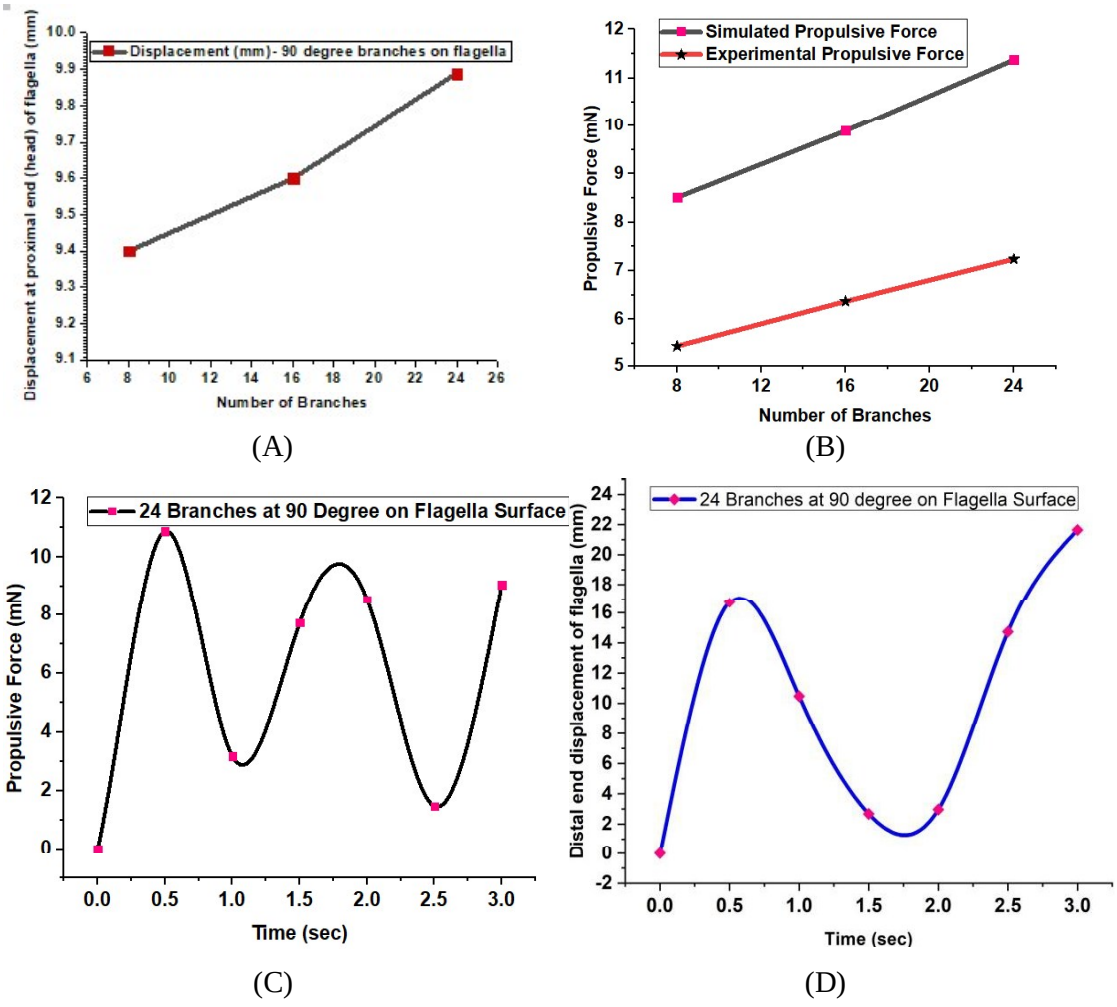

Figure 4.27 (A) Showing effect of increase in number of branches at 90° and 60° on flagella surface by measuring proximal end displacement of flagella head, (B) Simulated propulsive force value at flagella head for 8, 16 and 24 branches at 90° on flagella surface in comparison with experimental propulsive force value, (C) Propulsive Force at proximal end of flagella surface for 24 branched flagella and (D) Distal end displacement of flagella for 24 branches at 90° on flagella Surface.

Maximum propulsive force observed for 24 branched flagellated swimmer is 11.37 mN which is comparable to propulsive force reported in literature for non-branched helical flagella in the range of 5.7 μN to 80 mN [17-22] and mentioned in Table 4.1.

The fluid velocity depends on viscosity of fluid medium. Figure 4.28(a) shows the Reynolds number of the branched flagellated swimmer less than 1. The branched flagellated swimmer undulates with velocity v_y inside stationary silicon oil medium filled box. The displacement of head and propulsive forces of modelled flagella are varied by changing the number of branches. More the number of branches, larger is the effective surface area, larger the propulsive forces. Figure 4.27(A) shows that a linear relationship exists between the number of branches from 8, 16 and 24 on generating displacement of flagella head while keeping viscosity of fluid medium and velocity of proximal end constant. The displacement generated due to increment in number of branches on flagella through FEM simulation using COMSOL@5.4 software is compared with the real time experimentation performed at macro scale with PDMS based branched flagellated swimmer. The branches are oriented at 90° with respect to flagella axis.

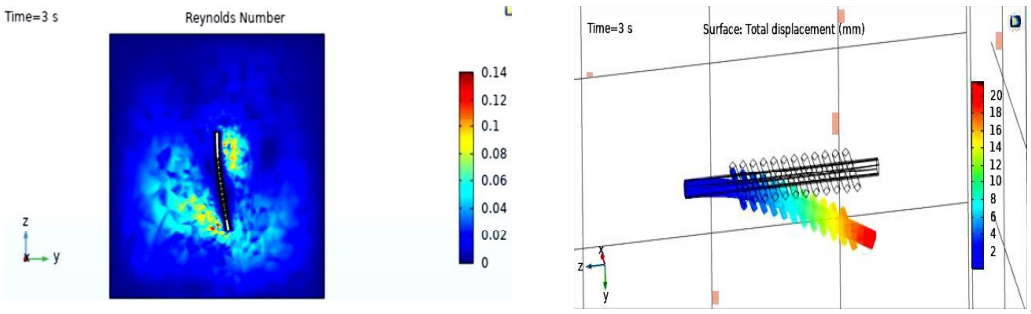

(a) (b)

Figure 4.28: (a) Reynolds number plot and (b) showing displacement of 24 branched flagellated swimmer

4.7 Summary

1. The flagellar arrangements exist in nature is described briefly in section 4.1. In section 4.2 macro-scale flagellum design reported in literature is discussed.
2. In section 4.3 literatures on mastigonemes bearing flagella is explained along with finite element modelling attempted for mastigonemes bearing flagella.
3. In section 4.4 experimental investigations on different designs of branches oriented at 90° is performed to see higher propulsive force generation. Numbers of branches,

orientation of branches (90°, 60° and 120°) and spacing between branches are considered and also compared its substantiality in terms of propulsive characteristics. In section 4.4.4, effect of gap in between branches are discussed and investigated experimentally.

4. In section 4.5, parametric optimization for branched flagellated swimmer is done using Taguchi analysis (DOE). Two techniques Taguchi and Pareto ANOVA analysis have been used and both illustrate similar inference. The branches are found to be most significant effect to produce maximum propulsive force. The practice of S/N ratio for selecting the best level of combination for propulsive force measurement value indicate higher value of speed of DC motor and viscosity of fluid medium to obtain better results. Taguchi method not only save the time and money but also developed the process. It has number of orthogonal array which emphasise main effects and facilitates the improvement in efficiency and reproducibility of small size experiments. After conducting the experiments, the deflection is recorded and S/N ratio is calculated for respective propulsive force calculated from deflection value. Through S/N ratio graph plotted, optimum parametric value is identified as speed of motor 500 RPM, Viscosity 20000cSt and number of branches 24.

5. In section 4.6, the experimental results for increase in number of branches from 8, 16 and 24 at 90° is validated through FEM simulation carried out in COMSOL Multiphysics software. More the number of branches lead to increase in propulsive force. Low Reynolds number is also maintained and shown in the graph.

References:

[1] Q. Wang, A. Suzuki, S. Mariconda, S. Porwollik, and R. M. Harshey, "Sensing wetness: a new role for the bacterial flagellum," *The EMBO journal*, vol. 24, no. 11, pp. 2034–2042, 2005.

[2] C. D. Silflow and P. A. Lefebvre, "Assembly and motility of eukaryotic cilia and flagella. Lessons from Chlamydomonas reinhardtii," *Plant physiology*, vol. 127, no. 4, pp. 1500–1507, 2001.

[3] H. C. Berg, "Feature Article Site Index Motile Behavior of Bacteria," *Physics today*, vol. 9, pp. 1–8, 2001.

[4] S. Namdeo, S. N. Khaderi, J. M. J. den Toonder, and P. R. Onck, "Swimming direction reversal of flagella through ciliary motion of mastigonemes," *Biomicrofluidics*, vol. 5, no. 3, pp. 34108-34124, 2011.

[5] H. C. Berg and D. A. Brown, "Chemotaxis in Escherichia coli analysed by three-dimensional tracking," *Nature*, vol. 239, no. 5374, pp. 500–504, 1972.

[6] T. Honda, K. I. Arai, and K. Ishiyama, "Micro swimming mechanisms propelled by external magnetic fields," *Magnetics, IEEE Transactions on*, vol. 32, no. 5, pp. 5085–5087, 1996.

[7] B. Behkam and M. Sitti, "Modeling and testing of a biomimetic flagellar propulsion method for microscale biomedical swimming robots," in *IEEE Advanced Intelligent Mechanotronics Conference, Monterey, CA*, pp. 24–28, 2005.

[8] S. Y. Tony, E. Lauga, and A. E. Hosoi, "Experimental investigations of elastic tail propulsion at low Reynolds number," *Physics of Fluids*, vol. 18, no. 9, pp. 91701-91705, 2006.

[9] G. Kósa, M. Shoham, and M. Zaaroor, "Propulsion method for swimming microrobots," *Robotics, IEEE Transactions on*, vol. 23, no. 1, pp. 137–150, 2007.

[10] G. Kósa *et al.*, "Flagellar swimming for medical micro robots: theory, experiments and application," in *2008 2nd IEEE RAS & EMBS International Conference on Biomedical Robotics and Biomechatronics*, pp. 258–263, 2008.

[11] N. Coq, O. Du Roure, M. Fermigier, and D. Bartolo, "Helical beating of an actuated elastic filament," *Journal of Physics: Condensed Matter*, vol. 21, no. 20, p. 204109-204116, 2009.

[12] N. S. Ha and N. S. Goo, "Development of a biomimetic swimmer," in *World Automation Congress (WAC)*, pp. 1–6, 2010.

[13] T. W. R. Fountain, P. V Kailat, and J. J. Abbott, "Wireless control of magnetic helical microrobots using a rotating-permanent-magnet manipulator," in *Robotics and Automation (ICRA), IEEE International Conference on*, pp. 576–581, 2010.

[14] J. Singleton, E. Diller, T. Andersen, S. Regnier, and M. Sitti, "Micro-scale propulsion using multiple flexible artificial flagella," in *Intelligent Robots and Systems (IROS), IEEE/RSJ International Conference on*, pp. 1687–1692, 2011.

[15] F. Z. Temel and S. Yesilyurt, "Magnetically actuated micro swimming of bio-inspired robots in mini channels," in *IEEE International Conference on*

Mechatronics, pp. 342–347, 2011.

[16] T. Xu, G. Hwang, N. Andreff, and S. Régnier, "Modeling and swimming property characterizations of scaled-up helical microswimmers," *IEEE/ASME Transactions on Mechatronics*, vol. 19, no. 3, pp. 1069–1079, 2014.

[17] Z. Ye, S. Régnier, and M. Sitti, "Rotating Magnetic Miniature Swimming Robots With Multiple Flexible Flagella," *IEEE Transactions on Robotics*, vol. 30, no. 1, pp. 3–13, 2014.

[18] F. Z. Temel and S. Yesilyurt, "Confined swimming of bio-inspired microrobots in rectangular channels," *Bioinspiration & biomimetics*, vol. 10, no. 1, pp. 16015–16029, 2015.

[19] L. Wang, H. Xu, W. Zhai, B. Huang, and W. Rong, "Design and Characterization of Magnetically Actuated Helical Swimmers at Submillimeter-scale," *Journal of Bionic Engineering*, vol. 14, no. 1, pp. 26–33, 2017.

[20] G. Kósa *et al.*, "Flagellar swimming for medical micro robots: theory, experiments and application," in *Biomedical Robotics and Biomechatronics. BioRob. 2nd IEEE RAS & EMBS International Conference on*, pp. 258–263, 2008.

[21] A. G. Erman and S. Yesilyurt, "Swimming of onboard-powered autonomous robots in viscous fluid filled channels," in *Mechatronics (ICM), IEEE International Conference on*, pp. 348–353, 2011.

[22] B. Rodenborn, C.-H. Chen, H. L. Swinney, B. Liu, and H. P. Zhang, "Propulsion of microorganisms by a helical flagellum," *Proceedings of the National Academy of Sciences*, vol. 110, no. 5, pp. E338–E347, 2013.

[23] U. Danis, R. Rasooli, C.-Y. Chen, O. Dur, M. Sitti, and K. Pekkan, "Thrust and Hydrodynamic Efficiency of the Bundled Flagella," *Micromachines*, vol. 10, no. 7, pp. 449–470, 2019.

[24] and N. N. S. Shivani Nain, Jitendra Singh Rathore, "Enhanced Locomotion of Branched Flagellated Nanoswimmer: Design, Simulation and Experimental Investigation," *Journal of Mechanical Science and Technology*, pp. 1–12, 2019.

[25] G. B. Bouck, "The structure, origin, isolation, and composition of the tubular mastigonemes of the Ochromonas flagellum," *The Journal of cell biology*, vol. 50, no. 2, pp. 362–384, 1971.

[26] T. L. Jahn, M. D. Lanman, and J. R. Fonseca, "The mechanism of locomotion of flagellates. II. Function of the mastigonemes of Ochromonas," *The Journal of Protozoology*, vol. 11, no. 3, pp. 291–296, 1964.

[27] D. L. Ringo, "Flagellar motion and fine structure of the flagellar apparatus in Chlamydomonas," *The Journal of cell biology*, vol. 33, no. 3, pp. 543–571, 1967.

[28] D. M. Cahill, M. Cope, and A. R. Hardham, "Thrust reversal by tubular mastigonemes: immunological evidence for a role of mastigonemes in forward motion of zoospores ofPhytophthora cinnamomi," *Protoplasma*, vol. 194, no. 1–2, pp. 18–28, 1996.

[29] S. Nakamura, G. Tanaka, T. Maeda, R. Kamiya, T. Matsunaga, and O. Nikaido, "Assembly and function of Chlamydomonas flagellar mastigonemes as probed with a monoclonal antibody," *Journal of cell science*, vol. 109, no. 1, pp. 57–62, 1996.

[30] G. B. Witman, K. Carlson, J. Berliner, and J. L. Rosenbaum, "Chlamydomonas flagella: I. Isolation and electrophoretic analysis of microtubules, matrix, membranes, and mastigonemes," *The Journal of Cell Biology*, vol. 54, no. 3, pp. 507–539, 1972.

[31] S. Tottori and B. J. Nelson, "Artificial helical microswimmers with mastigoneme-inspired appendages," *Biomicrofluidics*, vol. 7, no. 6, pp. 61101-61106, 2013.

[32] M. E. J. Holwill and M. A. Sleigh, "Propulsion by hispid flagella," *Journal of Experimental Biology*, vol. 47, no. 2, pp. 267–276, 1967.

[33] C. Brennen, "Locomotion of flagellates with mastigonemes," *Journal of Mechanochemistry and Cell Motility*, vol. 3, no. 3, pp. 207–217, 1975.

[34] S. Kobayashi, R. Watanabe, T. Oiwa, and H. Morikawa, "Computational study of micropropulsion mechanism in water modeled on flagellum with projecting mastigonemes," *Journal of Biomechanical Science and Engineering*, vol. 4, no. 1, pp. 11–22, 2009.

[35] H. Guo, J. Nawroth, Y. Ding, and E. Kanso, "Cilia beating patterns are not hydrodynamically optimal," *Physics of Fluids*, vol. 26, no. 9, pp. 91901-91913, 2014.

[36] P. Tierno, R. Golestanian, I. Pagonabarraga, and F. Sagués, "Magnetically actuated colloidal microswimmers," *The Journal of Physical Chemistry B*, vol. 112, no. 51, pp. 16525–16528, 2008.

[37] J. J. Abbott *et al.*, "How should microrobots swim?," *The international journal of Robotics Research*, vol. 28, no. 11–12, pp. 1434–1447, 2009.

[38] S. N. Khaderi, M. Baltussen, P. D. Anderson, D. Ioan, J. M. J. Den Toonder, and P. R. Onck, "Nature-inspired microfluidic propulsion using magnetic actuation," *Physical Review E*, vol. 79, no. 4, pp. 46304-46308, 2009.

[39] J. den Toonder *et al.*, "Artificial cilia for active micro-fluidic mixing," *Lab on a Chip*, vol. 8, no. 4, pp. 533–541, 2008.

[40] S. Tanaydin, "Robust design and analysis for quality engineering." Taylor & Francis Group, pp. 348–349, 1998.

This document was created with the Win2PDF “print to PDF” printer available at
http://www.win2pdf.com

This version of Win2PDF 10 is for evaluation and non-commercial use only.

This page will not be added after purchasing Win2PDF.

http://www.win2pdf.com/purchase/